NASA TECHNICAL NOTE

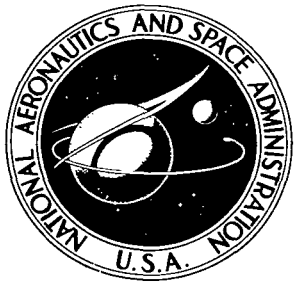

NASA TN D-6494

FAST NEUTRON REACTIVITY EFFECTS FOR REFRACTORY METALLIC SAMPLES MEASURED IN A THERMAL HOMOGENEOUS REACTOR

by Clarence R. Pierce, Daniel Fieno, and Donald F. Shook

Lewis Research Center
Cleveland, Ohio 44135

NATIONAL AERONAUTICS AND SPACE ADMINISTRATION • WASHINGTON, D. C. • SEPTEMBER 1971

1. Report No.	2. Government Accession No.	3. Recipient's Catalog No.
NASA TN D-6494		

4. Title and Subtitle
FAST NEUTRON REACTIVITY EFFECTS FOR REFRACTORY METALLIC SAMPLES MEASURED IN A THERMAL HOMOGENEOUS REACTOR

5. Report Date
September 1971

6. Performing Organization Code

7. Author(s)
Clarence R. Pierce, Daniel Fieno, and Donald F. Shook

8. Performing Organization Report No.
E-6198

10. Work Unit No.
129-02

9. Performing Organization Name and Address
Lewis Research Center
National Aeronautics and Space Administration
Cleveland, Ohio 44135

11. Contract or Grant No.

13. Type of Report and Period Covered
Technical Note

12. Sponsoring Agency Name and Address
National Aeronautics and Space Administration
Washington, D.C. 20546

14. Sponsoring Agency Code

15. Supplementary Notes

16. Abstract

Measurements and interpretations of fast-neutron reactivity effects have been made for metallic samples in a thermal uranyl fluoride - water-solution reactor. Experimental reactivity coefficients were obtained for a number of refractory metals enclosed by either a thick boron-10 shell or a cadmium shell located at the center of the cylindrical reactor. Calculated reactivities were obtained using a one-dimensional spherical model of the reactor and the multigroup S_n method. The measurements, along with the analytical procedure described, provide an integral test of fast-neutron cross sections. Measured and calculated epiboron effective absorption integrals are in agreement within the uncertainty of the measurement for tungsten, tantalum, and niobium; the calculated integral underestimated measured values for molybdenum by 35 percent and overestimated the measured values for rhenium by 65 percent.

17. Key Words (Suggested by Author(s))	18. Distribution Statement
Fast neutron reactivity; Refractory metals; Boron filter; Cadmium filter; Homogeneous reactor; Neutron absorption; Effective resonance integrals; Unresolved resonance parameters	Unclassified - unlimited

19. Security Classif. (of this report)	20. Security Classif. (of this page)	21. No. of Pages	22. Price*
Unclassified	Unclassified	26	$3.00

* For sale by the National Technical Information Service, Springfield, Virginia 22151

FAST NEUTRON REACTIVITY EFFECTS FOR REFRACTORY METALLIC SAMPLES MEASURED IN A THERMAL HOMOGENEOUS REACTOR

by Clarence R. Pierce, Daniel Fieno, and Donald F. Shook

Lewis Research Center

SUMMARY

The interpretation of reactivity effects of reactor materials in a fast-neutron environment has become increasingly important because of the technological emphasis on fast-breeder reactors and fast-reactor space-power systems. Quantitative difficulties are encountered in interpreting reactivity measurements made in fast reactors because of the large number of nuclides and the heterogeneity of the fast system. The present experiments were made to test the fast-neutron cross sections of metallic samples of interest to fast-spectrum reactors using a homogeneous thermal solution reactor.

Fast reactivity effects have been measured for tungsten, rhenium, tantalum, molybdenum, niobium, and lead in the NASA zero-power thermal solution reactor (ZP-II). Since there are no heterogeneity effects in the solution reactor, the calculations may be based on a model that closely approximates the reactor system.

A boron shell placed at the center of the solution reactor was used to produce a filtered central flux that is similar to that of a fast reactor. The large self-shielded metallic samples used further reduced the importance of low-energy neutron absorption compared with high-energy absorption and inelastic scattering. In addition, conventional cadmium covered measurements were made with the same samples as a check on the experimental procedure. These measurements showed that epicadmium effective resonance capture integrals of the large samples studied were in good agreement with available previously measured and calculated data.

The boron shell data were analyzed to determine epiboron effective absorption integrals for the metal samples exposed to the filtered fluxes within the boron shell. Measured epiboron effective absorption integrals agree with calculated integrals within the rather large experimental uncertainties for tungsten, tantalum, and niobium, but significant discrepancies were obtained for molybdenum and rhenium.

INTRODUCTION

Fast neutron reactivity effects have become a subject of increased study (ref. 1) because of the technological emphasis on fast-breeder reactors for commercial power generation and on fast-reactor space-power systems. Measurements of reactivity effects of samples using fast-spectrum reactors have been difficult to interpret because of uncertainties in the fast-neutron spectrum, the effects of material heterogeneity, and the large number of nuclides present. The present experiments were made to test the fast cross sections of refractory metallic samples of interest to fast space-power reactors.

Fast reactivity effects have been measured in a fully enriched uranyl fluoride - water-solution reactor. Since this solution reactor has a thermal spectrum, a boron-10 (^{10}B) filter is used to produce the fast-neutron flux environment for samples placed within the filter. The ^{10}B filter is a thick cylindrical shell with the center of the enclosed volume located at the center of the solution reactor. The large thermal and intermediate neutron energy absorption cross sections of ^{10}B reduce the central flux to negligible values for neutron energies below about 200 electron volts, and the central flux is considerably reduced for energies up to several kiloelectron volts.

The refractory metals, tungsten, rhenium, tantalum, molybdenum, and niobium were used for these measurements. Lead was used to estimate the inelastic scattering effects. Calculations were made to determine the various components of the sample reactivity effects that are due to the various neutron reactions that occur for each sample. There are no heterogeneity effects or nuclides of uncertain cross sections in the solution reactor; therefore, from these considerations, the calculations may be based on a model that closely approximates the experiment. From considerations of avoiding two-dimensional transport calculations, the cylindrical homogeneous reactor has been represented analytically as an equivalent sphere.

The measurements provide for integral tests of the absorption and inelastic scattering cross sections of the refractory metals above the kiloelectron-volt region. Epiboron effective absorption integrals that are obtained from the reactivity measurements are compared with corresponding values calculated using available cross sections.

Epicadmium effective resonance capture integrals of tungsten, rhenium, and tantalum have been measured previously for samples comparable to the samples used within the boron shell. As a check on the consistency of the experimental procedures used, the samples measured in the boron shell were also measured in a cadmium shell, and effective resonance capture integrals so obtained are compared with previously published values.

EXPERIMENT

The measurements were made in the NASA ZP-II, which is a uranyl fluoride-water thermal solution reactor (ref. 2). The reactor used for this study is shown in figure 1. The uranium content of the fuel was enriched to 93.2 percent uranium-235, and the fuel solution had a hydrogen to uranium-235 atom ratio of 1600. The diameter of the vessel is 76.3 centimeters, and the solution height of the critical reactor for this fuel solution is about 72 centimeters without the ^{10}B or cadmium shells in place. Criticality was controlled solely by means of solution height, which was measured using a remotely operated micrometer lead screw connected to an electric probe. The solution height for the critical reactor was about 86 centimeters with the ^{10}B shell and 83 centimeters with the cadmium shell centrally located. The reactor was unreflected for these measurements. A full description of the reactor may be found in reference 2.

Description of Samples

Sample information is shown in table I. Two measurements were made for each sample in the boron shell. Two measurements were made for the elements in the cadmium shell, with the exception of tantalum and lead. One measurement was made for tantalum in the cadmium shell, and four measurements were made for lead. An average of the measurements was made for each metal in the cadmium shell and for each metal in the boron shell. These averages were used for the analysis and in the presentation of results.

The tungsten samples used for both cadmium and boron shell measurements were made by filling the shell containers with microspheres of natural tungsten metal. The average sample density was 11.4 grams per cubic centimeters. Metal powder was used for the rhenium and tantalum samples, with an average sample density of 3.2 grams per cubic centimeter for rhenium and 4.6 grams per cubic centimeter for tantalum. The molybdenum sample for the boron shield experiment was a cylinder of the natural metal, 5.26 centimeter diameter and 6.35 centimeters high, with a weight of 1.349 kilograms.

A niobium sample of sufficient size was not available for the cadmium shell experiment. For the boron shell, a niobium bar with a nearly rectangular cross section was used, 4.42 by 3.51 centimeters, and 6.35 centimeters high, with a surface area of 128 square centimeters and a weight of 0.830 kilogram. A high-purity (99.992 percent) lead sample was used with the cadmium shell. The main impurities were antimony and tin (0.005 percent). The lead sample was a cylinder, 5.52 centimeters in diameter and 7.49 centimeters high, and weighed 2.058 kilograms.

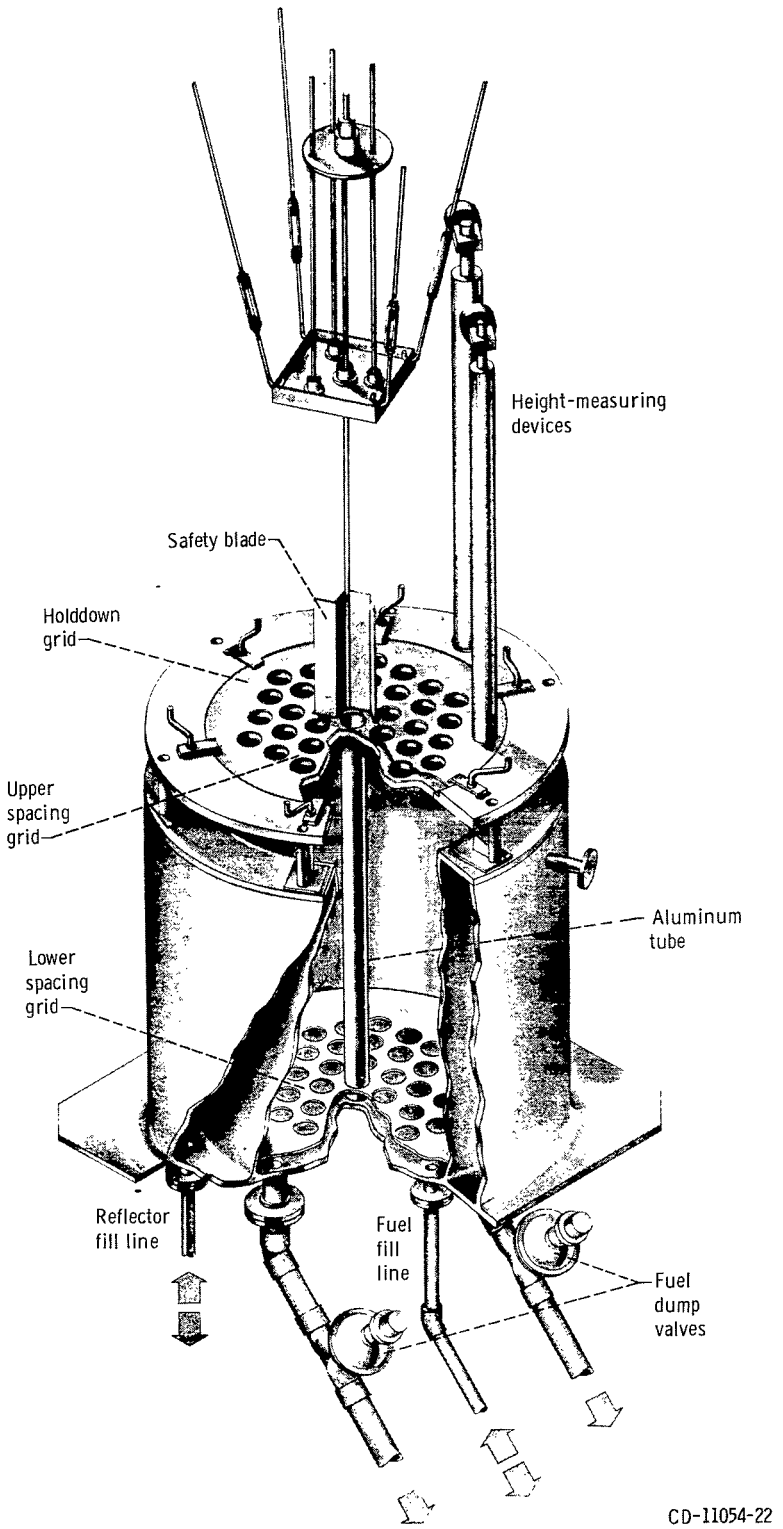

Figure 1. - NASA ZP-11, showing aluminum tube in center for positioning of samples.

TABLE I. - DESCRIPTION OF SAMPLES

Material	Form	Particle size	Density g/cm^3	Weight, g	Shape	Sample size, $(S/M)^{1/2}$ $cm/g^{1/2}$
			Cadmium shell			
Tungsten:						
Sample 1	Microsphere	400 μm	12.2	2478	Cylinder	0.28
Sample 2	Microsphere	400 μm	11.3	2255	↓	.29
Rhenium:						
Sample 1	Powder	220 Mesh	2.8	559	↓	.58
Sample 2	Powder	220 Mesh	2.9	580	↓	.57
Tantalum	Powder	325 Mesh	4.9	1024	↓	.44
Molybdenum:					↓	
Sample 1	Powder	325 Mesh	3.5	696	↓	.52
Sample 2	Powder	325 Mesh	3.5	709	↓	.52
Lead	Solid	---	11.5	2058	↓	.29
			Boron-10 shell			
Tungsten:						
Sample 1	Microsphere	400 μm	11.2	1477	Cylinder	0.31
Sample 2	Microsphere	400 μm	10.8	1566	↓	.31
Rhenium:					↓	
Sample 1	Powder	220 Mesh	3.5	510	↓	.53
Sample 2	Powder	220 Mesh	3.4	486	↓	.56
Tantalum:					↓	
Sample 1	Powder	325 Mesh	4.8	690	↓	.46
Sample 2	Powder	325 Mesh	4.0	584	↓	.51
Molybdenum	Solid	---	9.8	1349	↓	.33
Niobium	Solid	---	8.5	830	Rectangular bar	.39

Sample Holders

The measurements were made with the ^{10}B or cadmium filtered sample supported at the center of the fuel solution, within the aluminum tube shown in figure 1. The tube was slotted to permit fuel solution to enter above and below the sample. Boron powder enriched to 92 percent ^{10}B was compacted to a density of 1.4 grams per cubic centimeter and sealed within the walls and within the cap of the double walled cylindrical stainless-steel container shown in figure 2. The maximum particle size of the uncompacted powder was about 2.5 micrometers. The stainless-steel walls were 0.76 millimeter thick; the boron thickness was 6.35 millimeters. The 5.26-centimeter-inside-diameter inner cylinder was 6.67 centimeters high. The shells were held in place by

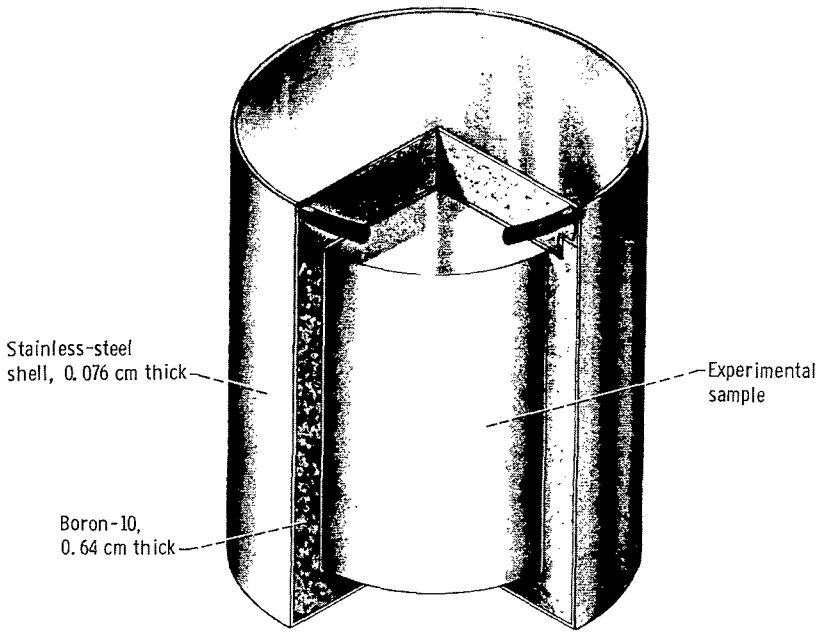

Figure 2. - Boron-10 filtered reactivity experiment sample holder.

plastic hold-down and support tubes (fig. 3). The solution height for the critical reactor was about 86 centimeters for the centrally located boron shell.

The cadmium container of 1.27 millimeter wall thickness, was held inside an O-ring sealed Lucite cylinder. The cadmium holder had a 6.10-centimeter inside diameter and was 7.62 centimeters high. The solution height for the critical reactor was about 83 centimeters for the centrally located cadmium shell.

Experimental Method

The quantities measured in this experiment are the reactivities of the refractory metals. The reactivities were determined by measuring the critical height with the empty shell at the center of the reactor and measuring the critical height again with the sample in the shell. Subject to small corrections for gradual fuel solution evaporation and variations in fuel solution temperature, the difference between the two critical heights (ΔH) is proportional to the reactivity of the sample, since ΔH is very small

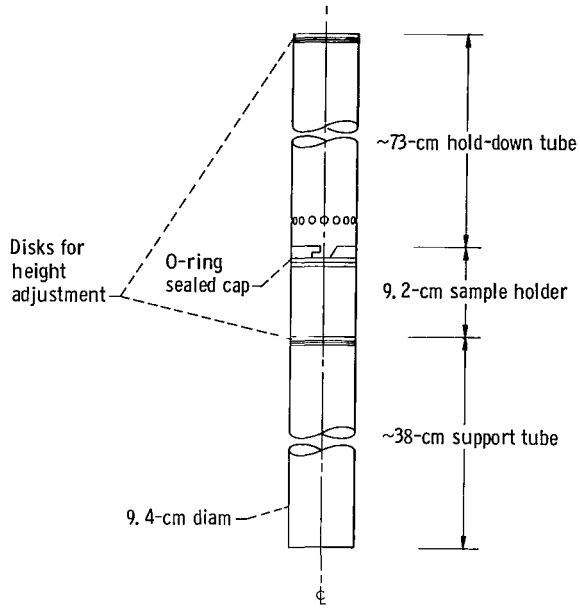

Figure 3. - Sample holder assembly for cadmium covered experiment.

compared with the total fuel height (ref. 3). With the fuel height measuring device used, relative heights could be determined to ±0.005 millimeter. This corresponds to reactivities of ±0.008 cent for the reactors used here.

The slow response of the reactor to small changes in solution height and the gradual fuel solution evaporation rate affect the precision of a critical height measurement. It is estimated that the corrected critical reactor fuel heights were determined to within about ±0.08 millimeter, which is equivalent to a reactivity of ±0.13 cent.

Corrections for gradual changes in critical height that are caused by small fuel-solution temperature changes were made by using an experimentally determined temperature coefficient of reactivity of 2.97 millimeters ΔH per K. This correction was especially significant for the boron shield data, since the solution temperature varied as much as 0.28 K on one of the days on which the boron shield measurements were made.

The reactivity correction for evaporation was obtained by redetermining the critical height for the empty shell in the reactor, after the first measurements for the empty shell and the shell with sample had been made. After corrections for room-temperature variations are applied, the difference between the empty-shell critical heights divided by the elapsed time yields the average evaporation rate. The reactivity correction for evaporation varied from day to day with reactor room relative humidity. Efforts were made to reduce the evaporation rate by enclosing the reactor in a plastic shroud and increasing the humidity within the shroud. These efforts reduced the evaporation rate from about 0.7 to roughly 0.3 millimeter ΔH per hour. It was necessary on occasion

to add small amounts of water to the fuel solution to maintain a constant hydrogen to uranium atom ratio.

METHOD OF ANALYSIS

Multigroup Calculations

Multigroup calculations using the S_n formulation of the neutron transport equation were used to obtain the real and adjoint fluxes for the reactor with empty ^{10}B or cadmium shells. In the interest of avoiding two-dimensional transport calculations, an equivalent one-dimensional spherical representation of the cylindrical (76.2-cm-diam and ~85 cm high) solution reactor is used for the calculations. The assumption made for this large reactor is that, if sufficient fuel solution surrounds the thick ^{10}B shell, then the spatial and energy distributions of the real and adjoint flux spectra within the shell should be similar for the spherical and cylindrical solution reactors. The radius of the sphere was chosen so that the reactor was critical with the empty shell in place.

The reactivity caused by a sample in the ^{10}B shell results in a small change in the radius of the critical spherical system. Similarly, in the cylindrical solution reactor, a sample placed in the ^{10}B shell would cause a perturbation in the reactor height to maintain criticality. These considerations suggest that calculations based on a spherical model of the cylindrical solution reactor may yield spectral and reactivity results comparable to those from a more complex two-dimensional cylindrical model. It will be seen that comparison of experimental and calculated epicadmium reactivity coefficients using the spherical model consistently underestimates the experimental coefficients by 15 percent, suggesting this as a bias present in the spherical calculations.

Thirty energy groups were used to describe the reactor spectra. The energy boundaries of the group split were chosen to provide detailed representation of fast neutron leakage and inelastic neutron scattering effects. The group structure is presented in table II. The thermal group (group 30) extends from 0.001 to 0.414 electron volt.

Two computer codes, GAM II (ref. 4) and GATHER II (ref. 5), were used to provide the necessary group-averaged microscopic cross sections. GAM II was used to calculate cross sections for the 29 fast groups. GATHER II was used to obtain thermal, or 30th group, cross sections. Both of these codes generated group-averaged microscopic cross sections for the uranyl fluoride - water solution having a hydrogen to uranium-235 atom ratio of 1600. Microscopic group cross sections were averaged over the spectra obtained for this fuel solution for ^{10}B, cadmium, and the test materials. These cross sections included the P_1 component of the elastic scattering kernel. For

TABLE II. - ENERGY AND LETHARGY BOUNDARIES

FOR THIRTY GROUP SPLIT

Group	Upper energy boundary, eV (a)	Upper lethargy boundary, eV	Group width (lethargy)
1	1.492×10^{7}	-0.4	0.4
2	1.000	0	.3
3	7.408×10^{6}	.3	↓
4	5.488	.6	↓
5	4.066	.9	↓
6	3.012	1.2	↓
7	2.231	1.5	↓
8	1.653	1.8	↓
9	1.225	2.1	↓
10	9.072×10^{5}	2.4	↓
11	6.721	2.7	↓
12	4.979	3.0	↓
13	3.688	3.3	↓
14	2.732	3.6	↓
15	2.024	3.9	↓
16	1.500	4.2	↓
17	1.111	4.5	.5
18	6.738×10^{4}	5.0	1.0
19	2.479	6.0	↓
20	9.119×10^{3}	7.0	↓
21	3.355	8.0	↓
22	1.234	9.0	↓
23	4.540×10^{2}	10.0	↓
24	1.670	11.0	↓
25	.61442	12.0	↓
26	.22603	13.0	↓
27	.08315	14.0	↓
28	.03059	15.0	↓
29	.01125	16.0	↓
30	.00414	17.0	---

[a]Bottom energy boundary is 0.001 eV for group 30.

the fuel solutions, the cross sections included a one-group upscattering component. These calculations are made using the S_4 approximation to the transport equation with the elastic scattering kernel treated through the P_1 order.

Reactivity Analysis

Equations. - The effective resonance capture integral I_{eff} for a sample in a neutron slowing down medium is defined as the energy-integrated capture cross section times the $1/E$ flux that yields the correct capture rate when the sample is exposed to the unperturbed flux spectrum that would be present in the absence of the sample. For the case of a very thin sample, I_{eff} is the dilute resonance integral and is related to the energy-dependent microscopic capture cross section $\sigma_c(E)$ (in barns) in the following way:

$$I_{eff} = \int_{E_{Cd}}^{\infty} \sigma_c(E) \frac{dE}{E} \tag{1}$$

where the slowing down flux in the surrounding medium varies inversely with neutron energy E and where E_{Cd} is an effective cadmium-cutoff energy of approximately 0.5 electron volt.

For a thick sample or lump of material, the flux distribution changes so that I_{eff} depends on a volume integral of the product of the actual flux in the sample and the capture cross section:

$$NV\varphi_0 I_{eff} = \int_{E_{Cd}}^{\infty} \int_V N\sigma_c(E)\varphi(E, \vec{r})\, dE\, d\vec{r} \tag{2}$$

where N is the sample atom density (in (atoms/cm^3)$\times 10^{-24}$), V is the sample volume (in cm^3) and φ_0 is the total unperturbed flux. It is implicit in equation (2) that the flux per unit energy $\phi(E)$ varies as $1/E$ when the thick sample is not present; therefore, equation (2) reduces to equation (1) for thin samples. The lower limit of the energy integrals in equations (1) and (2) represent a standardization of what is to be measured for a cadmium-covered sample; the value of E_{Cd} used here is 0.5 electron volt.

The reactivity $\Delta K/K$ of a cadmium-covered purely absorptive sample located at the center of a reactor is given by perturbation theory (ref. 6) as

$$\frac{\Delta K}{K} = \frac{-\int_{E_{Cd}}^{\infty} \int_{V} N\sigma_c(E)\, \varphi\,(E,\vec{r})\, \varphi^*\,(E,\vec{r})\, dE\, d\vec{r}}{f_{tot}} \tag{3}$$

where $\varphi^*(E,\vec{r})$ is the unperturbed adjoint function at the sample and f_{tot} is related to the total fission rate in the reactor.

In a thermal reactor, $\varphi(E)$ varies closely as $1/E$ in the resonance region of interest, while $\varphi^*(E)$ is nearly constant. Since E_{Cd} is approximately 0.5 electron volt, equation (3) can be rewritten using equation (2) as

$$\frac{\Delta K}{NVK} = - CI_{eff} \tag{4}$$

in equation (4), the constants f_{tot}, φ_0, and φ^* are combined into the constant C, and $\Delta K/NVK$ is the reactivity coefficient for the resonance absorber. The proportionality expressed by equation (4) permits the reactivity coefficients of unknown resonance absorbers to be related to effective resonance integrals by using an isotope with a known resonance integral as a standard to determine the constant C.

The following phenomena in the present reactivity measurements are of importance, particularly in the case of the boron filter:

(1) Departure of the reactor flux $\varphi(E)$ from a $1/E$ variation

(2) Variation of the adjoint function $\varphi^*(E)$ from constancy.

Adjustments for these effects for the cadmium filter were made by using calculated multigroup transport fluxes and adjoint functions for the perturbed reactor containing a cadmium cover and were applied by rewriting equation (4) as follows:

$$\frac{\Delta K}{NVK} = - CI_{eff} \left[\frac{\sum_i I_{eff,i}^{calc}\ \varphi_i(E)\varphi_i^*(E)}{I_{eff}^{calc}} \right] \tag{5}$$

The bracketed term in equation (5) is a small calculated multigroup importance correction factor to the measured reactivity coefficients that accounts for the actual values of $\varphi(E)$ and $\varphi^*(E)$ in the reactor (see ref. 3). Here $I_{eff,i}^{calc}$ is the calculated contribution

to the resonance integral for the energy group i; $\varphi_i(E)$ and $\varphi_i^*(E)$ are the calculated real and adjoint fluxes, respectively, for the energy group i.

For the boron-filtered sample, the quantity expressing the total fast reactivity coefficient is

$$-\frac{\Delta K}{NVKC} = \int_0^\infty \sigma_c(E)\varphi(E)\varphi^*(E)\,dE \tag{6}$$

The total experimental fast-reactivity coefficient is obtained from the measured value of the sample reactivity and is compared with the comparable analytical quantity (the flux weighted integral) in the numerator of equation (5). The constant of proportionality C is assumed to be unchanged.

Determination of I_{eff}. - The computer codes ZUT-TUZ (ref. 7) and GAROL (ref. 8) were used in computing I_{eff}. For computing I_{eff}, the GAROL code was used for the 1/v contribution to the effective resonance integral. The GAROL code was also used for calculating the resonance integral at energies greater than 10 kiloelectron volts with measured average cross sections as input. The codes ZUT and GAROL were used for the resolved resonance energy regions using the latest published resonance parameters. The unresolved resonance s-wave contributions were computed using the TUZ code. The sphere geometry option was used.

Effect of sample shape on the I_{eff} calculation: The codes permit calculations to be made for either spherical samples, infinite cylinders, or infinite slabs. Although there is no geometry option that matches the sample shapes (finite cylindrical and finite rectangular bar) used in the present experiment, a comparison of results for all three geometries is used to obtain an estimate of the geometry factor. The effect of sample geometry is of interest not only for the direct comparison with the one-dimensional transport calculation but also for the evaluation of the precision of input neutron capture cross sections.

As an example, the effective resonance integrals of tantalum, for a sample size within the range used in the present experiment, was calculated using the ZUT computer code for the three geometries available in the codes. The results are shown in table III and have been divided into two energy-group contributions. There are only small differences in the calculated effective resonance integrals for the infinite slab, infinite cylinder, and the sphere for the limited range of sample sizes covered in this report. Experiments have indicated that the finite cylinder case lies between that of the infinite slab and the infinite cylinder for equal sample surface-to-mass ratio, S/M (ref. 9). Calculations of collision probabilities, the quantities of importance in computing I_{eff} in ZUT and GAROL, have been made for the finite cylinder and the cuboid (ref. 10).

TABLE III. - CALCULATED EFFECTIVE RESONANCE INTEGRAL FOR TANTALUM

[Sample size, $(S/M)^{1/2}$, 0.347 $cm/g^{1/2}$]

Energy range, eV	Effective resonance integral, b		
	Slab geometry	Cylindrical geometry	Sphere geometry
0.5 - 500	32.30	32.73	32.84
500 - 1000	2.41	2.43	2.43
Total	34.71	35.16	35.27

These calculations show a maximum difference of about 4 percent between the collision probability for the finite cylinder and for the sphere at equal S/M values corresponding to an infinite cylinder radius of 1 centimeter.

The niobium sample may be approximated by a cuboid with the same S/M. When this is done, the difference in the collision probability for the sphere and for a cuboid is about 6 percent. Because of the insensitivity of I_{eff} to sample shapes the self-shielding for the samples measured may be calculated using any of the shapes provided for in the codes; the sphere geometry has been used.

Cross sections for tungsten: The resonance parameters and cross sections used to calculate the integral values for tungsten were those of references 3 and 11. The cross sections above 100 keV were those reported in reference 12.

Cross sections for rhenium: The resonance parameters used for the calculated integral values for rhenium were those of reference 13. This reference was also used for the cross sections in the unresolved region and above.

Cross sections for tantalum and molybdenum: The resonance parameters and cross sections for tantalum were obtained from reference 11. Resonance parameters for molybdenum were obtained from references 14 and 15. The high-energy cross sections were obtained from reference 14. Although molybdenum has many p-wave resonances at low energy, these resonances are weak, and their contribution to the effective resonance integral is small. (This was checked for in the calculations for niobium and is discussed there.) Hence, the ZUT and GAROL codes were used for the calculations, with all resonances considered as s-wave resonances. For the unresolved region calculation, the s-wave portion was evaluated using the TUZ code, and the p-wave contribution was estimated using measured average capture cross sections and the GAROL code. At high energy, the p-wave absorption is more significant than the s-wave.

Cross sections and calculations for niobium: Resonance parameters for niobium were obtained from references 14, 16, and 17. The effective resonance integrals were

calculated as described for molybdenum. Since niobium contains more resolved p-wave resonances than molybdenum, the effect of treating all resonances as s-wave was evaluated using the GAROL code and a 1/E flux in the moderating region. The known p-wave resonances were separated from the s-wave resonances and one "isotope" was simulated to have near zero potential scattering cross section and was assigned the p-wave resonances and another "isotope" was assigned the measured potential scattering cross section for niobium with the s-wave resonances. The mixed isotopes were run in the GAROL code. All resonances were then treated as being s-wave, and were lumped together in a single isotope. The GAROL result for the effective resonance integral was very nearly the same for both cases. The integrals were calculated for a range of $(S/M)^{1/2}$ from 0.39 centimeter per gram$^{1/2}$ used in the present experiment, to infinitely dilute. Calculated thick sample cadmium covered values were compared with thick sample values for niobium measured by Hellstrand (ref. 18) and were in good agreement with those values. The present calculations yield a dilute value of 9.04 barns, which is fairly close to the dilute value of 8.15±0.65 barns obtained by Hellstrand.

Real and adjoint flux weighting of I_{eff}. - Table IV shows the effect of flux weighting the calculated effective resonance integral. Relative values for the real and adjoint fluxes are used. For calculating the flux weighted integral for the cadmium covered case, the quantity $\varphi(E)\varphi^*(E)$ has been normalized to unity in the low-energy region of resolved resonances. This same normalization factor has been applied to the flux in the case of the boron shell. The 30 groups used in the calculation have been reduced to 10 groups in table IV for clarity. The third column lists the real flux times adjoint flux for each group for the boron shell. The calculated real flux and adjoint flux within the boron shell are shown in figure 4. The second column lists the same for the cadmium shell. The fourth and fifth columns list the contributions to the effective resonance integral for the various groups, for the cadmium shell tantalum sample and boron shell tantalum sample, respectively. Because of the different sizes of the cadmium and boron containers, the sample sizes were different for the two experiments. The sixth column lists the contributions to the dilute integral, and the last two columns list the effective resonance integral contributions multiplied by the corresponding real flux and adjoint flux. The fluxes within the boron shell are effectively zero over the energy region where the resonance integral contribution is largest. For equal lethargy intervals, the resonances in the keV region have the greatest effect on the flux within the boron shell.

Determination of the proportionality constant, C. - The proportionality constant C (eq. (4)) was obtained by using a measured value of I_{eff} for tungsten (ref. 3) along with a corresponding experimental value of the reactivity. The effective resonance integrals of tungsten have been measured for a wide range of sample sizes and therefore are used as secondary standards here. The value of C for the cadmium shell experiment also

TABLE IV. - FLUX WEIGHTED CROSS SECTION INTEGRALS FOR TANTALUM

Energy group, eV	Flux times adjoint flux		Effective resonance integral, I_{eff}, b		Dilute integral, I_{∞}, b	Flux weighted cross section integral, $I_{eff}^{\varphi\varphi^*}$, b	
	Cadmium shell	Boron shell	Cadmium shell (a)	Boron shell (b)		Cadmium shell	Boron shell
0.414 - 3.06	0.48	0	7.48	-----	5.50	3.59	0
3.06 - 61.4	1.02	0	19.79	-----	640.69	20.19	0
61.4 - 454	1.10	.01	9.94	11.12	66.70	10.92	.11
454 - 9119	1.22	.17	7.13	7.64	16.75	8.70	1.30
9.12 - 24.8×10^3	1.37	.57	1.09	1.11	3.20	1.49	.63
24.8 - 150×10^3	1.72	.96	.83	.84	.86	1.43	.81
150 - 907×10^3	3.82	2.77	.39	.40	.41	1.49	1.11
0.91 - 2.23×10^6	4.77	3.92	.09	.09	.09	.43	.35
2.23 - 5.49×10^6	6.67	5.67	.03	.03	.03	.20	.17
5.49 - 10.0×10^6	1.63	1.50	0	0	0	0	0
				Total	734.25	48.45	4.48

[a]Sample size, $(S/M)^{1/2}$, 0.44 $cm/g^{1/2}$.
[b]Sample size, $(S/M)^{1/2}$, 0.49 $cm/g^{1/2}$.

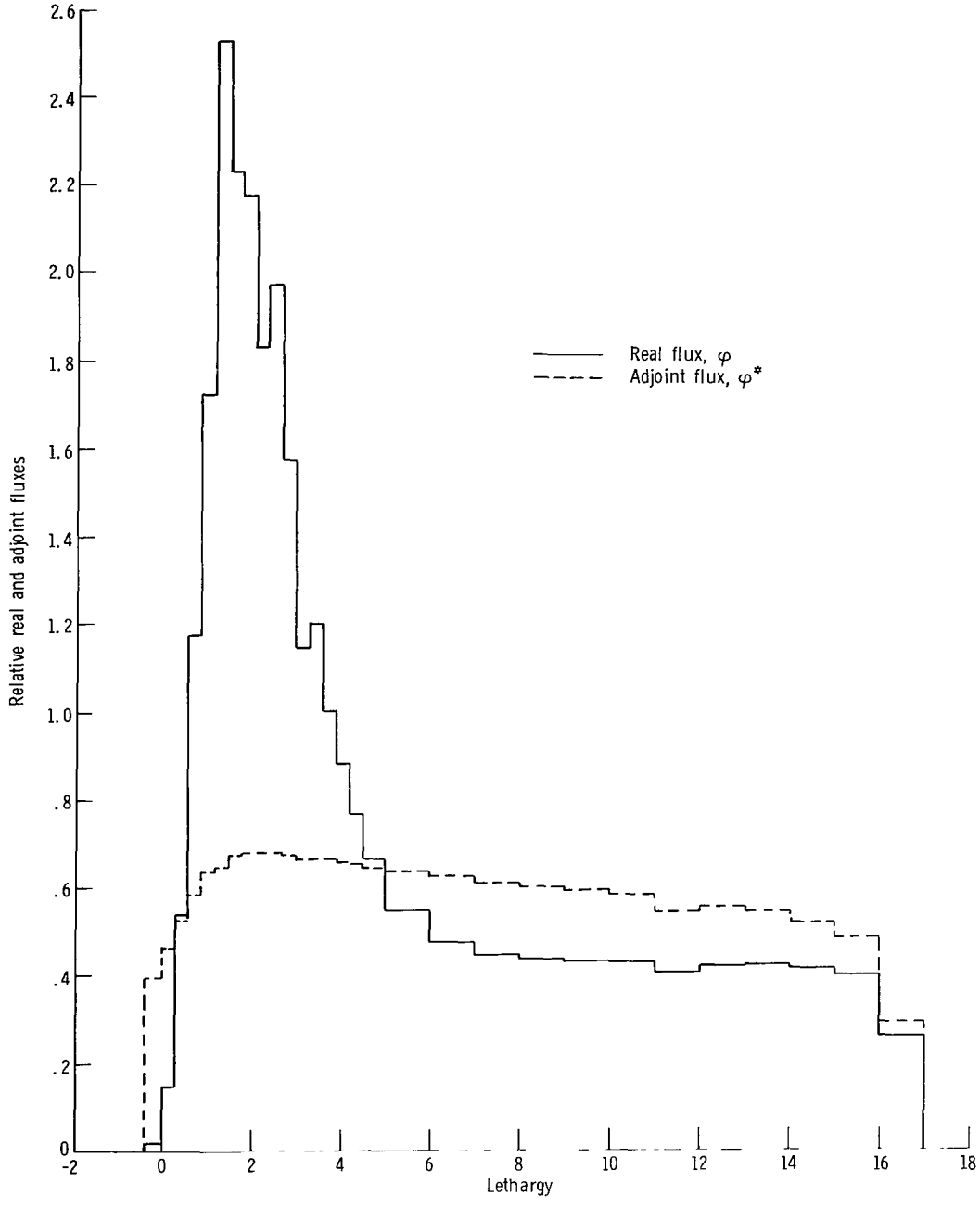

(a) In cadmium shell.

Figure 4. - ZP-II central flux and adjoint flux.

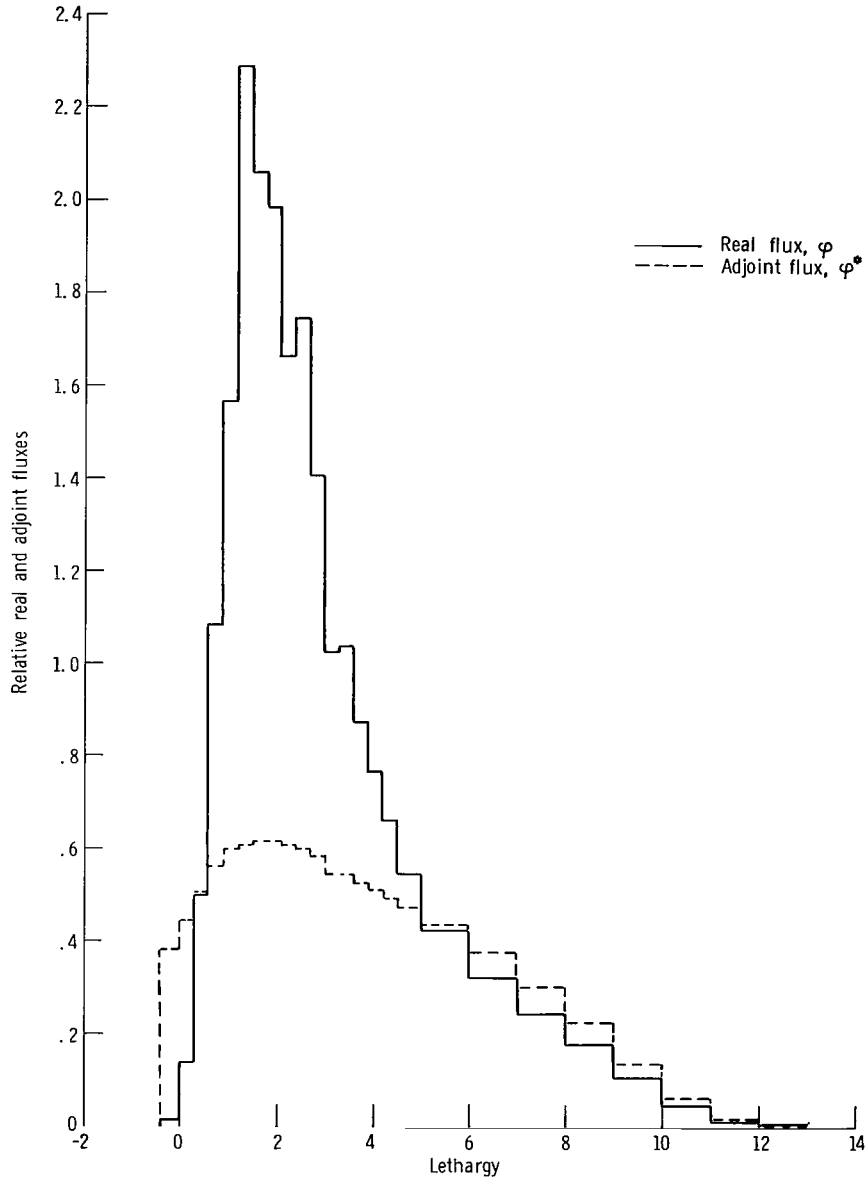

(b) In boron-10 shell.

Figure 4. - Concluded.

was used for samples in the boron shell and was found to give agreement with calculated values of the integral flux weighted cross section or fast reactivity coefficient for most samples within the boron shell.

Inelastic scattering and other reactivity components. - Interactions contributing to the reactivity of the sample in addition to radiative capture include elastic and inelastic scattering and (n, 2n) reactions. The elastic and (n, 2n) contributions are very small compared with the capture and inelastic component. The calculated inelastic contribution is nearly 50 percent of the total reactivity of some of the boron-filtered samples. The calculated inelastic coefficients are computed using inelastic cross sections from the GAM-II data tape.

Table V shows the calculated contributions to the reactivity for the elements investigated. Listed are the absorption and inelastic effects and the total reactivity, all in cents. The inelastic contribution is small compared with the total contribution for the cadmium shell samples, but it is a major fraction of the total contribution for the boron shell samples. Inelastic scattering is the major contributor to the reactivity of the lead sample. Lead was used as a standard so that a measured effect of inelastic scattering could be compared with the calculated effect. The inelastic components are all positive for the cadmium shell samples, and negative for the boron shell samples. The calcu-

TABLE V. - CALCULATED NEUTRON ABSORPTION AND INELASTIC SCATTERING CONTRIBUTIONS TO THE REACTIVITY OF SAMPLES IN ZPR-II

[Effective delayed neutron fraction, β_{eff}, 0.00695.]

Sample	Reactivity, cents				
	Absorption	Inelastic scattering	Elastic scattering	(n, 2n)	Total
Cadmium shell					
Tungsten	-11.95	0.44	-0.18	0.08	-11.61
Rhenium	-14.01	.14	-.02	.02	-13.87
Tantalum	-12.45	.17	-.03	.03	-12.28
Molybdenum	-2.30	.25	-.05	.01	-2.09
Lead	-.03	.39	-.05	.04	.35
Boron shell					
Tungsten	-0.52	-0.59	-0.05	0.04	-1.12
Rhenium	-.91	-.13	-.01	.01	-1.04
Tantalum	-.52	-.33	-.01	.01	-.85
Molybdenum	-.56	-.49	-.11	.02	-1.14
Niobium	-.66	-.43	-.10	.01	-1.18

lated inelastic scattering cross-section contribution was subtracted from the measured total reactivity to obtain the measured absorption reactivity values; thus the measured absorption values for the boron shell samples depend, to a large extent, on the precision of the inelastic scattering cross sections.

Corrections for evaporation and temperature. - Measurements of molybdenum are used to illustrate the magnitude of the fuel solution evaporation and temperature corrections to the sample critical height differences ΔH. The ΔH values and the corrections are shown in table VI for both the cadmium shell samples and the boron shell sample.

TABLE VI. - RELATIVE MAGNITUDE OF CORRECTIONS FOR MOLYBDENUM

Shell	Run	Temperature correction, ΔH, mm	Evaporation correction, ΔH, mm	Corrected ΔH, mm	Corrected $\Delta H/NV$, mm$\times 10^{-24}$ atoms
Cadmium	1	-0.23	0.82	1.72	0.394
	2	-.66	1.07	1.64	.368
Boron	1	-0.26	1.05	1.31	0.155
	2	-.68	2.19	.88	.104

The last column in table VI gives the corrected critical reactor height difference divided by the number of atoms of sample, NV, times 10^{-24}. All runs shown were made on different days. Although the applied corrections are large relative to ΔH, fair agreement between runs is obtained for the cadmium filtered samples. Most cadmium-filtered runs, made with the same material, yielded values within 10 percent of each other. The values for the boron shell were within about 40-percent agreement on the average. The large temperature and evaporation corrections for run 2 for molybdenum with the boron shell was the result of a long period between empty shell runs. The experimental errors reported here are based on the uncertainties in the critical height determinations.

RESULTS AND DISCUSSION

Calculated and measured reactivities for the metals studied are tabulated and compared. The calculated and measured flux-weighted effective resonance integrals are tabulated and compared.

Comparison of total reactivity coefficients. - Calculated and measured reactivity coefficients are shown in table VII for both cadmium-filtered and boron-filtered samples.

TABLE VII. - CALCULATED AND EXPERIMENTAL TOTAL

REACTIVITY COEFFICIENTS

Element	Sample size, $(S/M)^{1/2}$, $cm/g^{1/2}$	Reactivity coefficient for Cd-filtered sample, (cents/g)×10^3		Reactivity coefficient for ^{10}B-filtered sample, (cents/g)×10^3	
		Measured	Calculated	Measured	Calculated
Tungsten	0.29	-5.66±0.03	-4.91	----------	------
	.31	----------	-----	-0.87±0.22	-0.740
Rhenium	.58	-29.0±1.5	-24.4	----------	------
	.54	----------	-----	-1.88±0.70	-2.10
Tantalum	.44	-13.4±0.61	-12.0	----------	------
	.51	----------	-----	-1.55±0.61	-1.33
Molybdenum	.52	-3.75±0.42	-2.93	----------	------
	.33	----------	-----	-1.35±0.31	-.84
Niobium	.39	----------	-----	1.18±0.43	-1.42
Lead	.294	+0.14±0.14	+0.17	----------	------

The measured and calculated values for the cadmium-filtered samples shown in table VII agree within about 15 percent, with all the calculated values consistently below the error limits of the measured values for the cadmium-filtered samples. If all the calculated reactivities for the cadmium-filtered samples were increased by 15 percent, complete agreement would be obtained within the error limits. This underestimate could be a calculational bias due to the geometry difference between the spherical model used in the S_n calculation and the cylindrical reactor used for the measurements.

For the boron-filtered samples, the measured and calculated values agree with the exception of molybdenum, where the calculated value is nearly 40 percent smaller than the measured value. Table VII shows that, for these reactors, the epiboron reactivity coefficient of tungsten is the lowest of all the refractory metals covered in this study.

Comparison of epicadmium and epiboron effective capture integrals. - Table VIII shows the measured and calculated effective resonance capture integrals weighted by the fluxes within the cadmium and boron shells for the metals studied here. The calculated quantities shown in this table represent the numerator in equation (5). All the epicadmium calculated values are in good agreement with the measured values. The epiboron effective capture integrals are in reasonable agreement for tungsten, tantalum, and niobium within the estimated error limits. The calculated value for molybdenum is 35 percent smaller than the measured value, and the measured value for rhenium is 65 percent smaller than the calculated value. Tables VII and VIII indicate that the high-energy absorption cross sections used in the calculations for molybdenum may be too

TABLE VIII. - MEASURED AND CALCULATED EPICADMIUM AND EPIBORON EFFECTIVE CAPTURE INTEGRALS

Element	Sample size, $(S/M)^{1/2}$, $cm/g^{1/2}$	Effective capture integral, $\sum_i (I_{eff})_i^{calc} \varphi_i \varphi_i^*$			
		Cadmium shell, b		Boron shell, b	
		Measured	Calculated	Measured	Calculated
Tungsten	0.29	21±2	22.06	-------	----
	.31	-------	------	1.7±0.8	1.63
Rhenium	.58	106±12	101.8	-------	----
	.54	-------	------	5.8±2.5	9.7
Tantalum	.44	48±5	47.05	-------	----
	.51	-------	------	3.7±2.0	4.58
Molybdenum	.52	7.6±1.1	7.65	-------	----
	.33	-------	------	1.6±0.5	1.04
Niobium	.39	-------	------	1.0±0.7	1.38

low, since the calculated values for the boron shell in both tables lie below the error limit of the measurement. An increase of 20 percent in capture cross section would produce agreement in both tables.

Figure 5 shows the measured and calculated effective resonance absorption integrals for tungsten, rhenium, tantalum, molybdenum, and niobium, respectively. Also shown are data obtained by previous measurement (refs. 3, 19, and 20) Measured and calculated epiboron effective capture integrals are shown on the same figures. The present measurement of the epicadmium tantalum effective resonance capture integral agrees well with the previous values.

The present measurement for the epiboron integral for rhenium is smaller than the calculated value by about 30 percent for one measurement and by about 50 percent for the other measurement. The large discrepancies for rhenium absorption cannot be due to uncertainty in the inelastic scattering component of the total reactivity. The calculated value for this component accounts for only 12 percent of the total calculated reactivity for the epiboron case. Its magnitude could be larger by a factor of 2 and not affect agreement within error limits between the calculated and total reactivities; therefore, the discrepancy observed for rhenium is due to errors in the input capture cross sections in the kilovolt region. The suspected low calculation of the epiboron integral for molybdenum is shown in figure 5(d). The measured and calculated values for tungsten, tantalum, and niobium are well within the estimated error limits of the measurement.

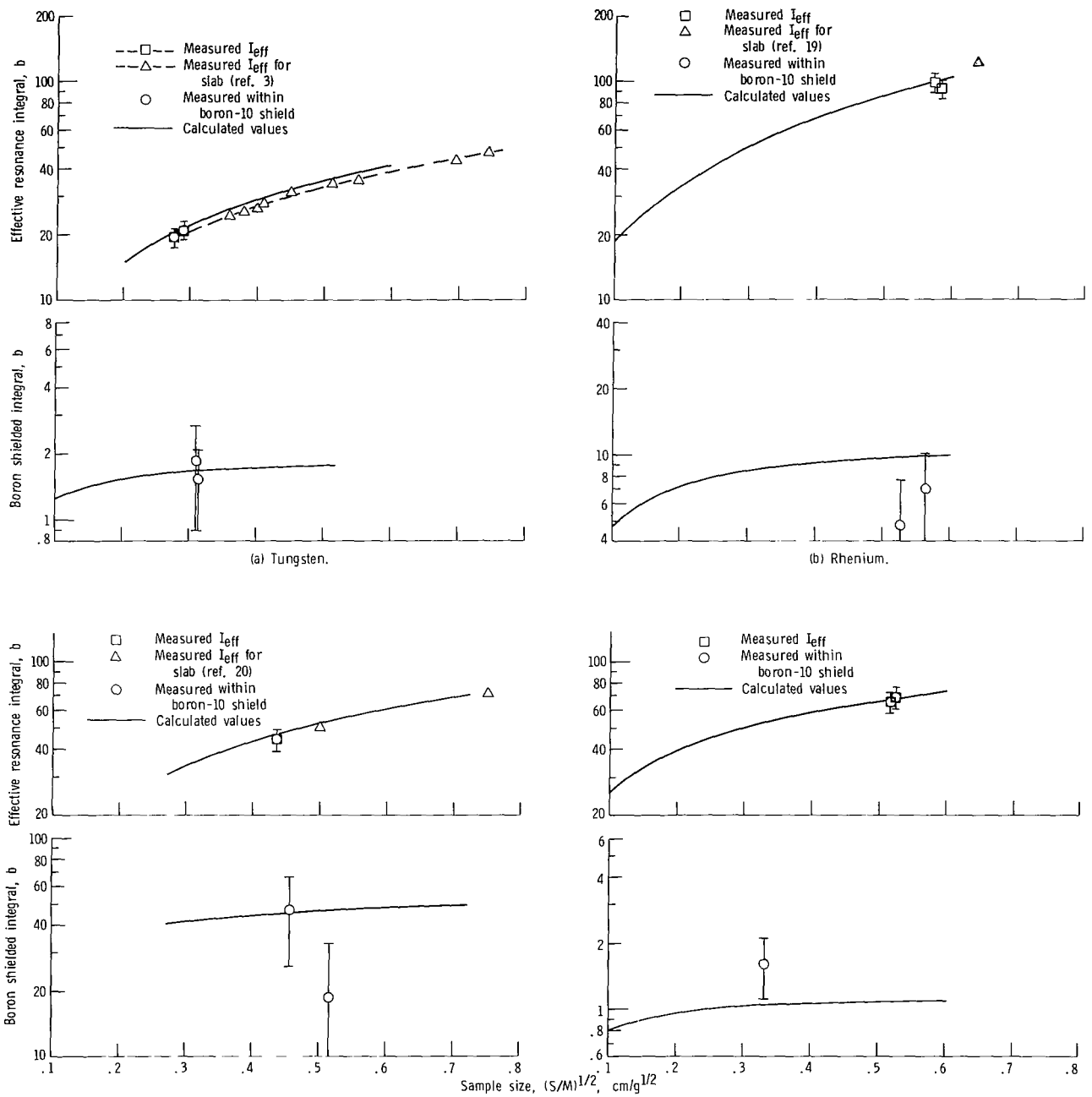

Figure 5. - Measured shielded value of $\int_0^\infty \sigma_{eff}\varphi\varphi^\circ \, dE$ compared with calculated value $\Sigma(I_{eff})_i r_i \varphi_i \varphi_i^\circ$ and measured I_{eff} compared with calculated I_{eff}.

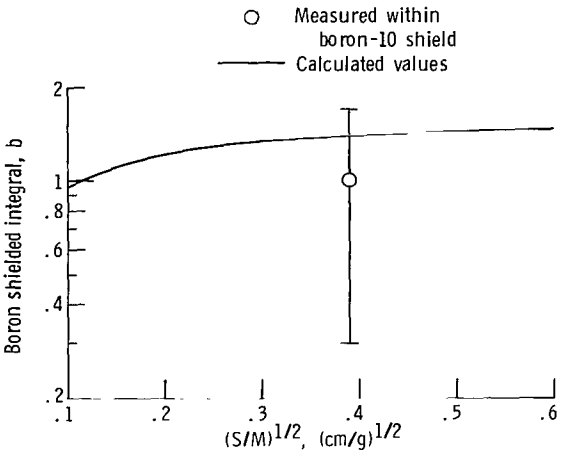

(e) Niobium.

Figure 5. - Concluded.

CONCLUDING REMARKS

Fast reactivity coefficients for tungsten, rhenium, tantalum, molybdenum, and niobium were measured using the NASA zero power reactor-II (ZP-II) and a boron-10 filter.

Measurements and calculations were also made using a cadmium filter to serve as a check on the use of NASA ZP-II for this type of experiment. The measured cadmium-filter reactivities were consistently 15 percent larger than the calculated values, which might be attributed to a bias in the transport calculations that employed a spherical reactor model rather than a two-dimensional cylindrical model. The measured and calculated reactivity coefficients agree within error limits for the boron-10 shielded samples of tungsten, tantalum, rhenium, and niobium. In the case of molybdenum, the calculation was 40 percent smaller than the measured value. Calculated effective resonance integrals were weighted by the flux within the boron shield and were compared with the boron-filtered data. Agreement was obtained for tungsten, tantalum, and niobium with discrepancies observed for molybdenum and rhenium. For molybdenum, the calculated epiboron integral was 35 percent below the measured value; the calculated epiboron integral for rhenium was 65 percent above the measured value.

Lewis Research Center,
National Aeronautics and Space Administration,
Cleveland, Ohio, June 25, 1971,
129-02.

REFERENCES

1. Davey, W. G.: Differential Data and the Interpretation of Large, Fast Reactor, Critical Experiment. Proceedings of the Conference on Neutron Cross Sections and Technology. D. T. Goldman, ed. NBS Spec. Publ. 299, vol. 2, National Bureau of Standards, 1968, p. 1211.

2. Fox, Thomas A.; Mueller, Robert A.; Ford, C. Hubbard; and Alger, Donald L.: Critical Mass Studies with NASA Zero Power Reactor II. I - Clean Homogeneous Configurations. NASA TN D-3097, 1965.

3. Shook, Donald F.; and Bogart, Donald: Effective Resonance Integrals of Separated Tungsten Isotopes from Reactivity Measurements. Nucl. Sci. Eng., vol. 31, no. 3, Mar. 1968, pp. 415-430.

4. Joanou, G. D.; and Dudek, J. S.: GAM-II. A B_3 Code for the Calculation of Fast-Neutron Spectra and Associated Multigroup Constants. Rep. GA-4265, General Dynamics Corp., Sept. 16, 1963.

5. Joanou, G. D.; Smith, C. V.; and Vieweg, H. A.: GATHER-II. An IBM-7090 Fortran-II Program for the Computation of Thermal-Neutron Spectra and Associated Multigroup Cross Sections. Rep. GA-4132, General Dynamics Corp., July 8, 1963.

6. Radkowsky, A., ed.: Naval Reactors Physics Handbook. Vol. 1: Selected Basic Techniques. USAEC Rep. TID-7030, 1964, ch. 5, pp. 864-869.

7. Kuncir, G. F.: A Program for the Calculation of Resonance Integrals. Rep. GA-2525, General Atomic Div., General Dynamics Corp., Aug. 28, 1961.

8. Stevens, C. A.; and Smith, C. V.: GAROL, A Computer Program for Evaluating Resonance Absorption, Including Resonance Overlap. Rep. GA-6637, General Atomic Div., General Dynamics Corp., Aug. 24, 1965.

9. Gilat, J.; and Gurfinkel, Y.: Self-Shielding in Activation Analysis. Nucleonics, vol. 21, no. 8, Aug. 1963, pp. 143-144.

10. Carlvik, I.: Collision Probabilities for Finite Cylinders and Cuboids. Nucl. Sci. Eng., vol. 30, no. 1, Oct. 1967, pp. 150-151.

11. Goldberg, Murrey D.; Mughabghab, Said F.; Purohit, Surendra N.; Magurno, Benjamin A.; and May, Victoria A.: Neutron Cross Sections. Vol. IIC. Z=61 to 87. Rep. BNL-325, 2nd ed., Suppl. 2, Vol. 2C, Brookhaven National Lab., Aug. 1966.

12. Fricke, M. P.; and Lopez, W. M.: Radiative Strength Function for Fast Neutron Capture. Phys. Letters, vol. 29B, no. 7, June 23, 1969, pp. 393-395.

13. Friesenhahn, S. J.; Gibbs, D. A.; Haddad, E.; Fröhner, F. H.; and Lopez, W. M.: Neutron Capture Cross Sections and Resonance Parameters of Rhenium from 0.01 eV to 30 keV. J. Nucl. Energy, vol. 22, no. 4, Apr. 1968, pp. 191-210.

14. Goldberg, Murrey D.; Mughabghab, Said F., Purohit, Surendra N.; Magurno, Benjamin A.; and May, Victoria M.: Neutron Cross Sections. Vol. IIB. Z=41 to 60. Rep. BNL-325, 2nd ed., Suppl. 2, Vol. 2B, Brookhaven National Lab., May. 1966.

15. Shwe, Hla; and Coté, R. E.: Neutron Resonances of Mo Isotopes. Phys. Rev., vol. 179, no. 4, Mar. 20, 1969, pp. 1148-1153.

16. Garg, J. B.; Rainwater, J.; and Havens, W. W., Jr.: Neutron Resonance Spectroscopy. V. Nb, Ag, I, and Cs. Phys. Rev., vol. 137, no. 3B, Feb. 8, 1965, pp. 547-575.

17. Lopez, W. M.; Haddad, E.; Friesenhahn, A. J.; and Fröhner, F. H.: Niobium Resonance Parameters. Nucl. Phys., vol. A93, 1967, pp. 340-356.

18. Hellstrand, E.; and Lundgren, G.: The Resonance Integral of Niobium. Rep. AE-81, AB Atomenergi, Sweden, Aug. 1962.

19. Pierce, Clarence R.; Shook, Donald F.; and Bogart, Donald: Resonance Integrals of Rhenium for a Wide Range of Sample Sizes. NASA TN D-4938, 1968.

20. Pierce, Clarence R.; Shook, Donald F.; and Bogart, Donald: Effective Resonance Integrals of Tantalum. NASA TN D-5628, 1970.

NASA-Langley, 1971 — 22 E-6198

"The aeronautical and space activities of the United States shall be conducted so as to contribute . . . to the expansion of human knowledge of phenomena in the atmosphere and space. The Administration shall provide for the widest practicable and appropriate dissemination of information concerning its activities and the results thereof."

— NATIONAL AERONAUTICS AND SPACE ACT OF 1958

NASA SCIENTIFIC AND TECHNICAL PUBLICATIONS

TECHNICAL REPORTS: Scientific and technical information considered important, complete, and a lasting contribution to existing knowledge.

TECHNICAL NOTES: Information less broad in scope but nevertheless of importance as a contribution to existing knowledge.

TECHNICAL MEMORANDUMS: Information receiving limited distribution because of preliminary data, security classification, or other reasons.

CONTRACTOR REPORTS: Scientific and technical information generated under a NASA contract or grant and considered an important contribution to existing knowledge.

TECHNICAL TRANSLATIONS: Information published in a foreign language considered to merit NASA distribution in English.

SPECIAL PUBLICATIONS: Information derived from or of value to NASA activities. Publications include conference proceedings, monographs, data compilations, handbooks, sourcebooks, and special bibliographies.

TECHNOLOGY UTILIZATION PUBLICATIONS: Information on technology used by NASA that may be of particular interest in commercial and other non-aerospace applications. Publications include Tech Briefs, Technology Utilization Reports and Technology Surveys.

Details on the availability of these publications may be obtained from:

SCIENTIFIC AND TECHNICAL INFORMATION OFFICE

NATIONAL AERONAUTICS AND SPACE ADMINISTRATION

Washington, D.C. 20546